Remote Sensing of Environment 112 (2008) 3898–3907

Contents lists available at ScienceDirect

Remote Sensing of Environment

journal homepage: www.elsevier.com/locate/rse

Influence of incidence angle on detecting flooded forests using C-HH synthetic aperture radar data

Megan W. Lang [a,*], Philip A. Townsend [b], Eric S. Kasischke [c]

[a] USDA Agricultural Research Service, Hydrology and Remote Sensing Lab Beltsville, Maryland, United States
[b] Department of Forest Ecology and Management, University of Wisconsin-Madison, United States
[c] University of Maryland, Department of Geography, United States

ARTICLE INFO

Article history:
Received 8 May 2006
Received in revised form 24 June 2008
Accepted 26 June 2008

Keywords:
Flooding
Forest
Hydrology
Hydropattern
Hydroperiod
Incidence angle
Inundation
Radar
Radarsat
Synthetic aperture radar
SAR
Swamp
Wetland

ABSTRACT

Hydrology is the single most important abiotic factor in the formation and functioning of a wetland. Many limitations still exist to accurately characterizing wetland hydrology over large spatial extents, especially in forested wetlands. Imaging radar has emerged as a viable tool for wetland flood mapping, although the limitations of radar data remain uncertain. The influence of incidence angle on the ability to detect flooding in different forest types was examined using C-HH Radarsat-1 data (23.5°, 27.5°, 33.5°, 39.0°, 43.5°, and 47.0°) during the leaf-off and leaf-on seasons. The ability to detect flooding under leaf-on conditions varied much more according to incidence angle while forest type (open canopy tupelo-cypress, tupelo-cypress, and bottomland hardwood) had a greater effect during the leaf-off season. When all forest types were considered together, backscatter generally decreased with increasing incidence angle under all conditions (2.45 dB between 23.5° and 47.0° flooded, leaf-off; 2.28 dB between 23.5° and 47.0° not flooded, leaf-off; 0.62 between 23.5° and 43.5° flooded, leaf-on; 1.73 dB between 23.5° and 43.5° not flooded, leaf-on; slope was not constant between incidence angles), but the distinction between flooded and non-flooded areas did not decline sharply with incidence angle. Differentiation of flooded and non-flooded forests was similar during the leaf-off and leaf-on seasons. The ability to detect inundation under forest canopies was less than expected at smaller incidence angles and greater than expected at larger incidence angles, based on the results of previous studies. Use of a wider range of incidence angles during the entire year increases the temporal resolution of imagery which may, in turn, enhance mapping of inundation beneath forest canopies.

Published by Elsevier Inc.

1. Introduction

Wetland hydropattern – spatial and temporal variations in inundation and soil saturation – is the primary factor controlling the formation of wetlands and is a major driver of ecosystems processes within wetlands. Small changes in water regime can cause large changes in wetland characteristics and functions (e.g., Mitsch & Gosselink, 2000). Although the importance of hydropattern is widely understood, analysis of inundation patterns across landscapes remains limited by the unavailability of *in situ* data due to the excessive expense needed to collect accurate ground-based information and the difficulty of modeling hydrology in areas of subtle topography (Hess et al., 1990, Townsend & Walsh 1998; Tiner, 1999). Current literature states that the hydrological sciences are limited by a lack of data (Engman, 1996; Conly and Van der Kamp, 2001; Mendoza et al., 2003; Price, 2005), especially long-term data at broad spatial scales. Remote sensing offers the potential to overcome such limitations, but traditional optical remote sensing methods are ineffective during times of the year when the ground is obscured by vegetation.

Imaging radar has emerged as a viable alternative to *in situ* data collection and temporally limited optical data for monitoring inundation in wetland ecosystems (Bourgeau-Chavez et al., 2005; Hess et al., 1990; Hess et al., 1995; Imhoff et al., 1987; Kasischke et al., 2003; Krohn et al., 1983; Ormsby et al., 1985; Townsend & Walsh 1998; Wang et al., 1995). However, the utility of synthetic aperture radar (SAR) data for this purpose has not been fully explored, and important questions remain regarding sensor and environmental conditions that may limit the ability of SAR to detect flooding beneath forest canopies. Specifically, incidence angle (the angle between the radar signal and an imaginary line perpendicular to the Earth's surface) can affect the utility of SAR data for monitoring inundation primarily due to interactions with the intervening canopy. Although the incidence angle effect has been modeled (Enheta & Elachi, 1982; McDonald et al., 1990; Richards et al., 1987; Wang et al., 1995) and some studies have been conducted (Ford & Casey 1988; Töyrä et al., 2001; Kandus et al., 2001), empirical evaluation is still limited. The objective of this paper is to determine the influence of incidence angle on the ability of C-HH SAR data to detect flooding under forest canopies. Radarsat-1 (C-HH) SAR data, collected at different incidence angles under leaf-on and leaf-off conditions, were evaluated

* Corresponding author.
E-mail address: Megan.Lang@ars.usda.gov (M.W. Lang).

0034-4257/$ – see front matter. Published by Elsevier Inc.
doi:10.1016/j.rse.2008.06.013

in a study region where these data have already been used to effectively map flooded forests (Townsend 2001).

2. Background

The potential of SAR data to benefit forested wetland research is substantial because of the sensitivity of microwave energy to the presence or absence of standing water and its ability to penetrate forest canopies, even during the leaf-on period (Hall 1996; Kasischke et al., 1997; Kasischke & Bourgeau-Chavez 1997; Rao et al., 1999). Because the analytical methods for interpretation are relatively new compared to optical remote sensing, research has been ongoing to fully develop the capabilities of imaging radars.

SARs are active sensors, using different wavelengths of microwave radiation and often transmitting and receiving that energy in different planes relative to the direction that the energy is traveling. Although a number of past studies have used L-band (15.0–30.0 cm wavelengths) data to study flooding beneath forest canopies (Hess et al., 1995; Krohn et al., 1983; Place, 1985; Pope et al., 1997; Townsend & Walsh 1998), there was a gap in the availability of L-band satellite data between 1998 (Japan Earth Resources Satellite) and 2006 (Phased Array Type L-band Synthetic Aperture Radar). This led researchers to assess the suitability of C-band (4.0–7.5 cm wavelengths) SAR data for forested wetland hydrology research. As more studies concluded that C-HH data could be used to accurately detect flooding beneath the forest canopy under certain conditions (Costa 2004; Townsend and Walsh 1998; Townsend, 2000), the need to fully define the limitations of these data increased.

Radar energy is typically transmitted at angles incident to the Earth's surface ranging from ~10° to ~65°, where small angles (closer to nadir) are considered steep incidence angles and larger angles are termed shallow. Many studies concluded that smaller incidence angles were preferable for distinguishing flooded from non-flooded forests (Bourgeau-Chavez et al., 2001; Ford & Casey 1988; Hess et al., 1990; Richards et al., 1987; Töyrä et al., 2001; Wang et al., 1995). Others have not shown incidence angle to affect the ability of SAR data to detect flooding beneath vegetation (Imhoff et al., 1986; Ormsby et al., 1985). Hess et al. (1990) concluded that the role of incidence angle in the ability of SAR to detect flooding beneath forest canopies should be further explored.

A simple model can be used to describe the interaction of microwave energy, transmitted by a SAR sensor towards the Earth's surface, with different elements that comprise the scattering surface. Forests are conceptualized as having three layers: The canopy layer, the trunk layer, and the ground layer, where total backscatter coefficient from a forest (σ^{o}) is described as (Kasischke and Bourgeau-Chavez 1997; Townsend 2002; Fig. 1):

$$\sigma^{o} = \sigma_{c}^{o} + \tau_{c}^{2}\tau_{t}^{2}\left(\sigma_{t}^{o} + \sigma_{s}^{o} + \sigma_{d}^{o} + \sigma_{m}^{o}\right) \quad (1)$$

where

- σ_{c}° backscatter coefficient of the crown layer of smaller woody branches and foliage,
- τ_{c} transmissivity of the crown layer,
- τ_{t} transmissivity of the trunk layer,
- σ_{t}° backscatter coefficient of the trunk layer,
- σ_{s}° backscatter coefficient of the surface layer,
- σ_{d}° double-bounce between the trunk and the surface layers, and
- σ_{m}° multi-path scattering between the ground and canopy layers.

Due to the size (usually 5–6 cm) of the microwave wavelength in relation to the size of smaller woody branches and foliage, C-band SAR total backscatter coefficient (σ°) is primarily influenced by scattering caused by the crown layer (σ_{c}°). However, in flooded forests double-bounce (σ_{d}°) and multi-path scattering (σ_{m}°) can have a sizable effect on total backscatter coefficient when the transmissivity of the crown (τ_{c}) and trunk (τ_{t}) layers is sufficiently high. In addition to greatly increasing double-bounce (σ_{d}°) and multi-path scattering (σ_{m}°), inundation beneath the forest canopy also eliminates surface scattering (σ_{s}°). Because of large increases in total backscatter coefficient (σ°) caused by inundation, flooded forests often have much higher total backscatter coefficient (σ°) than non-flooded forests. In non-flooded forests, increases in soil moisture raise surface backscatter coefficient (σ_{s}°) and multi-path scattering (σ_{m}°). However, the increase in double-bounce (σ_{d}°) and multi-path scattering (σ_{m}°) that flooding causes is much higher than the increase caused by higher soil moisture levels (Wang et al., 1995). Increases in canopy foliage leaf area index (LAI) during the warmer months decrease the transmissivity of the crown layer (τ_{c}), and thus decrease the amount of microwave energy reaching the forest floor. Therefore, an increase in foliage should reduce the ability to detect flooded forests using SAR data. More detailed explanations of microwave scattering from forests are found in Dobson et al. (1995) and Wang et al. (1995).

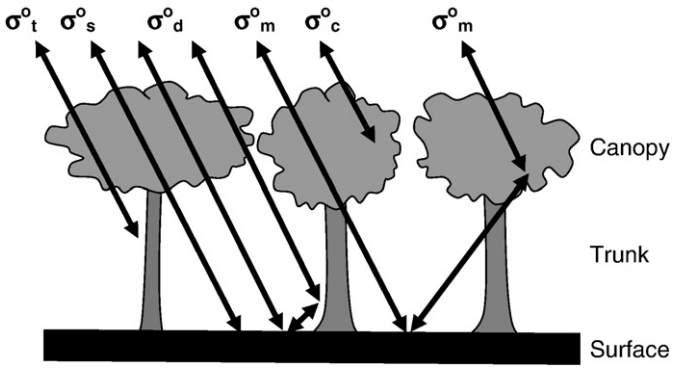

Fig. 1. Conceptual drawing of the major sources of backscatter from forests (σ_{c}°=backscatter coefficient of the crown layer of smaller woody branches and foliage; τ_{c}=transmissivity of the crown layer; τ_{t}=transmissivity of the trunk layer; σ_{t}°=backscatter coefficient of the trunk layer; σ_{s}°=backscatter coefficient of the surface layer; σ_{d}°=double-bounce between the trunk and the surface layers; and σ_{m}°=multi-path scattering between the ground and canopy layers; adapted from Kasischke & Bourgeau-Chavez, 1997).

The influence of incidence angle on backscatter varies according to forest structure (i.e., basal area, canopy height, canopy depth, and branching qualities) and ground layer characteristics, including surface roughness, soil moisture, and the presence/absence of standing water (Hess et al., 1990; Rauste, 1990). Much like forests are described as having specific spectral signatures using optical remote sensing, forests have distinct angular signatures (backscatter coefficient as a function of incidence angle) when imaged at multiple incidence angles (Rauste, 1990). Microwave energy that is transmitted by SARs operating at larger (shallower) incidence angles interacts more with the canopy, thus decreasing transmissivity in the crown layer (τ_{c}), but increasing the ability of the radar to estimate canopy characteristics (Kandus et al., 2001; Magagi et al., 2002; Rauste, 1990; Sun & Simonett, 1988). In contrast, microwave energy transmitted at smaller (steeper) incidence angles takes a shorter route through the canopy, increasing transmissivity in the crown layer (τ_{c}) and leaving more energy to interact with the trunk and ground layers.

Backscatter is expected to vary with incidence angle in flooded and non-flooded forests, under leaf-on and leaf-off conditions. The longer path length at shallow incidence angles generally increases attenuation in the canopy and therefore decreases backscatter coefficient originating from the ground surface (Hess et al., 1990; Kandus et al., 2001; Magagi et al., 2002; Rauste, 1990; Sun & Simonett, 1988). Backscatter from flooded and non-flooded sites should decrease with increasing incidence angle due to lower transmissivity in the crown and trunk layers. It is hypothesized, however, that the decrease will be greater for

flooded sites due to enhanced attenuation of multi-path and double-bounce scattering caused by the increasingly shallow (closer to the ground) return of the energy as it is reflected off the water surface (the return pathway of the energy is less direct). Therefore, while we expect backscatter coefficient to decrease with increasing incidence angle in both flooded and non-flooded forests (Hess et al., 1990; Magagi et al., 2002; Rauste, 1990; Sun & Simonett, 1988), we expect the decrease to be greater for flooded forests. As a consequence, the difference in backscatter coefficient between flooded and non-flooded forests should decrease with increasing incidence angle.

In leaf-off flooded forests greater transmissivity in the canopy layer should lead to higher backscatter coefficient relative to leaf-on flooded forests (Hess et al., 1990). We hypothesize that the difference between flooded and non-flooded sites will be greater during the leaf-off season as more microwave energy penetrates the crown layer and interacts with the ground.

3. Methods

Effect of incidence angle on the ability of C-HH SAR data to detect flooding was examined in three forest types (open tupelo-cypress [<50% canopy cover], tupelo-cypress [>50% canopy cover], and deciduous bottomland hardwood forests) during the winter (leaf-off) and summer (leaf-on). Backscatter coefficient was also examined in upland deciduous and pine forests for comparison with the floodplain forests. A flood simulation model (Townsend & Foster, 2002), derived independently from stream flow and radar data was used to distinguish areas of flooding from non-flooded areas. A digital map of vegetation cover (Townsend & Walsh, 2001) was then used to stratify forest types within Radarsat-1 SAR images with incidence angles from 20° to 49°. Average radar backscatter coefficient (σ°) from each forest type was compared in flooded and non-flooded areas using the multi-incidence angle data.

3.1. Study area

The study area is located in the Coastal Plain of northeastern North Carolina, including the lower Roanoke and much smaller Cashie Rivers, and covers some of the most expansive and pristine forested wetlands on the East Coast of the U.S. (Fig. 2). The Roanoke River originates in the Blue Ridge Mountains of Virginia and flows 209 km through the Blue Ridge, Piedmont, and Coastal Plain Physiographic Provinces before emptying into the Atlantic Ocean. The river's floodplain covers approximately 61,000 ha and varies in width between <5 and 10 km. The study area has a subtropical climate with lingering, humid summers and mild winters (average annual temperature of 15.5 °C). Annual precipitation averages 120 cm, and usually exceeds evapotranspiration, with most rain occurring during summer.

The area around the Roanoke River can be divided into two general geomorphic settings, floodplain and upland. Topographic variations at the study site are subtle. However, within the floodplain, even small changes in elevation lead to large differences in hydropattern. The meandering river channel is surrounded by depositional levees that decrease in elevation into backwater areas towards terraces or uplands on either side of the floodplain. Higher areas within the floodplain are often traversed by intermittent stream channels that serve as conduits into and out of backwater areas. Much of the floodplain is inundated some time during the year and backwater areas can remain flooded for

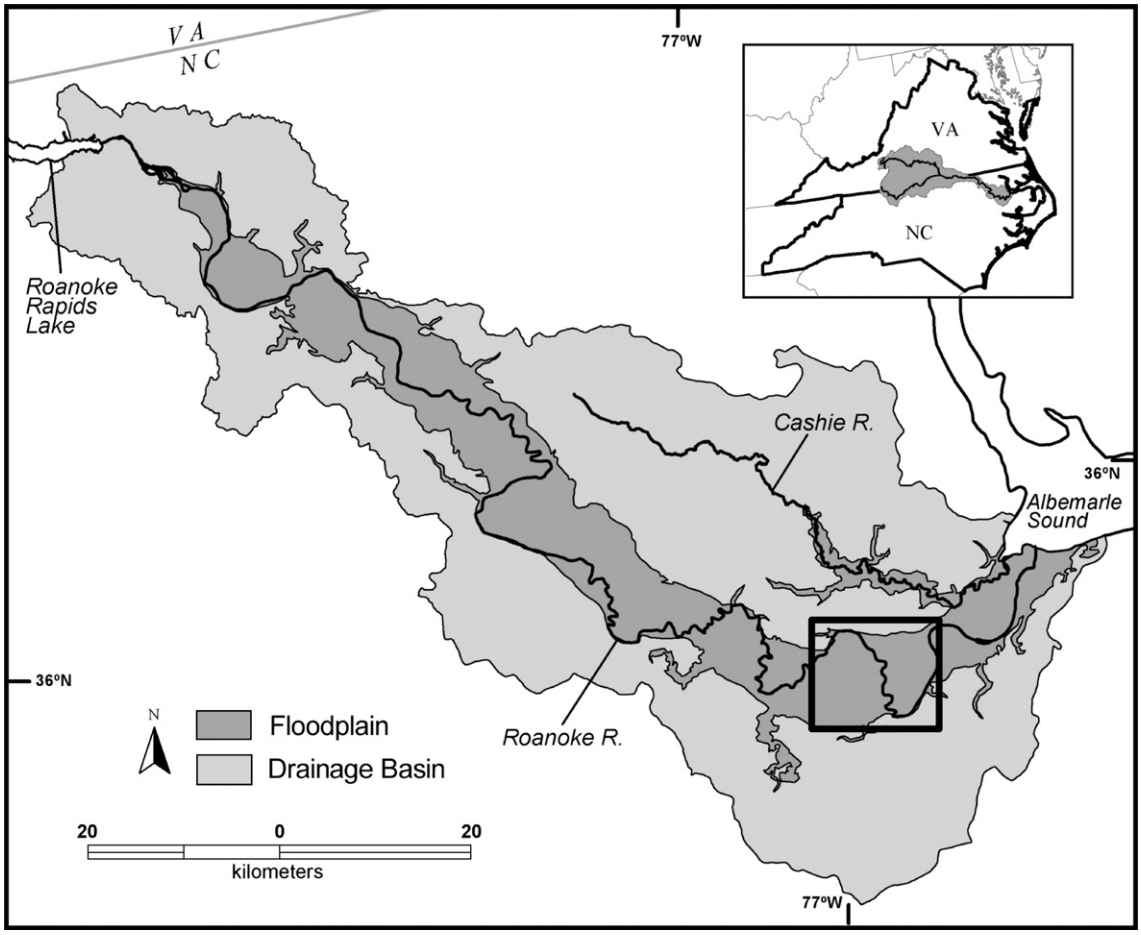

Fig. 2. Roanoke River Study Site, North Carolina, U.S.A. Areas illustrated in gray (floodplain and drainage basin) comprise the entire study site. The area depicted in Figs. 3, 4, and 5 is indicated by a box in the southeastern portion of the study site.

longer periods. As a result, tupelo-cypress (*Nyssa aquatica–Taxodium distichum*) forests dominate in backwater areas while a mixture of deciduous floodplain species are found in drier areas. Although cypress trees were more dominant in tupelo-cypress forests, their numbers have been reduced by selective logging and they now represent less than 30% of the canopy trees in tupelo-cypress forests (Townsend, 2002). The dominant trees in the mixed deciduous bottomland hardwood forests include: Red maple (*Acer rubrum*), green ash (*Fraxinus pennsylvanica*), sweet gum (*Liquidambar styraciflua*), oaks (*Quercus michauxii, Quercus lyrata, Quercus phellos,* and *Quercus laurifolia*), American elm (*Ulmus americana*), box elder (*Acer negundo*), and sugarberry (*Celtis laevigata*). Duration of flooding and subtlety of elevation generally increase downstream. Timing and duration of inundation is mainly controlled by variations in the amount of water released from upstream dams, with lesser controls including evapotranspiration, precipitation, soil texture, soil organic matter, and antecedent conditions (Townsend & Foster, 2002).

3.2. Data and analysis

Eleven standard beam Radarsat-1 (C-HH) images, collected in 2000, were analyzed, six leaf-off and five leaf-on. (Figs. 3 and 4 illustrate differences in backscatter between the 11 images in a small section of the study site, while Fig. 5 illustrates the type of forests found within the area depicted by Figs. 3 and 4.) The leaf-on images had incidence angles ranging from 20° to 46° and the leaf-off images had incidence angles between 20° and 49° (Table 1). Although incidence angle varies from near to far range (closer to and further from the sensor), it should be noted that the portion of the Roanoke River floodplain examined in this study extends across nearly the entire range direction of the image. Analysis of incidence angle as it varied from near to far range for all dates, forest types and flood conditions (i.e., flooded or non-flooded; Table 2) confirmed that average incidence angle for the entire image generally corresponded to the average incidence angle for test sites examined in this study (<1° or 2° difference for all forest types during all conditions and incident angles except for deciduous forests when observed with an average image incidence angle of 23.5° when it varied by 2.34°). Precipitation data were acquired for each image date from the National Oceanic and Atmospheric Administration's National Climatic Data Center (www.ncdc.noaa.gov) for the Williamston, North Carolina station (Table 1).

Before analysis, all SAR data were radiometrically calibrated, resampled to 30 m, and georeferenced to UTM coordinates using

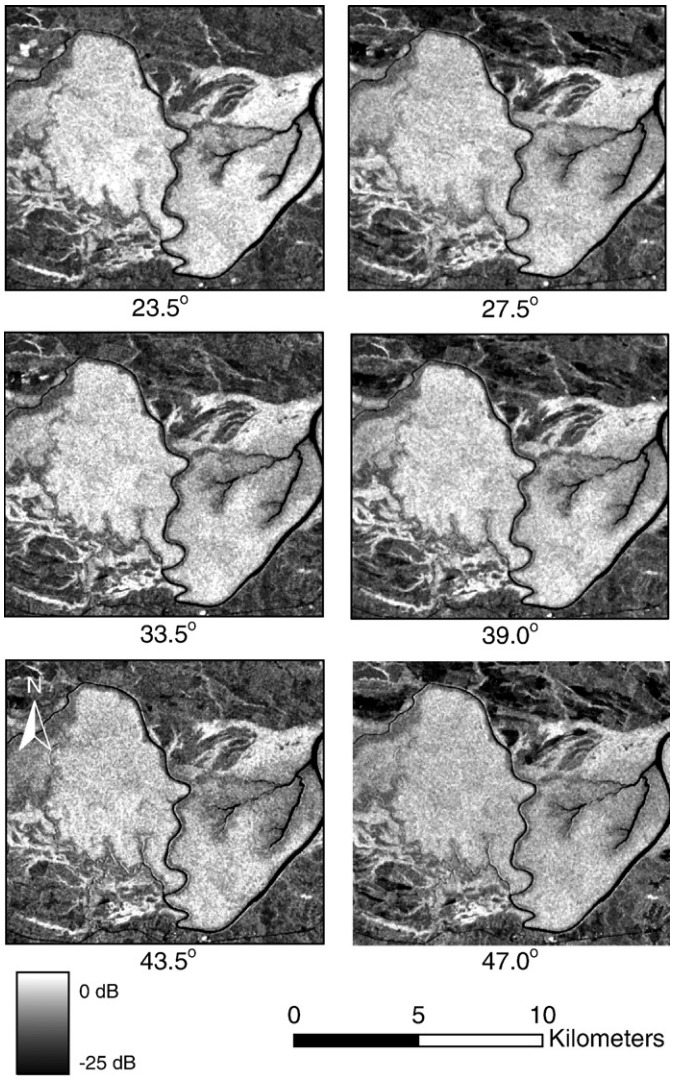

Fig. 3. A small portion of the leaf-off Radarsat-1 images in order of increasing incidence angle. All images are from December 2000, and were collected during a period of similar river discharge. Please see Fig. 2 for the location of this sample area relative to the entire study site. Pixel values ranged from 0 dB (white) to −25 dB (black).

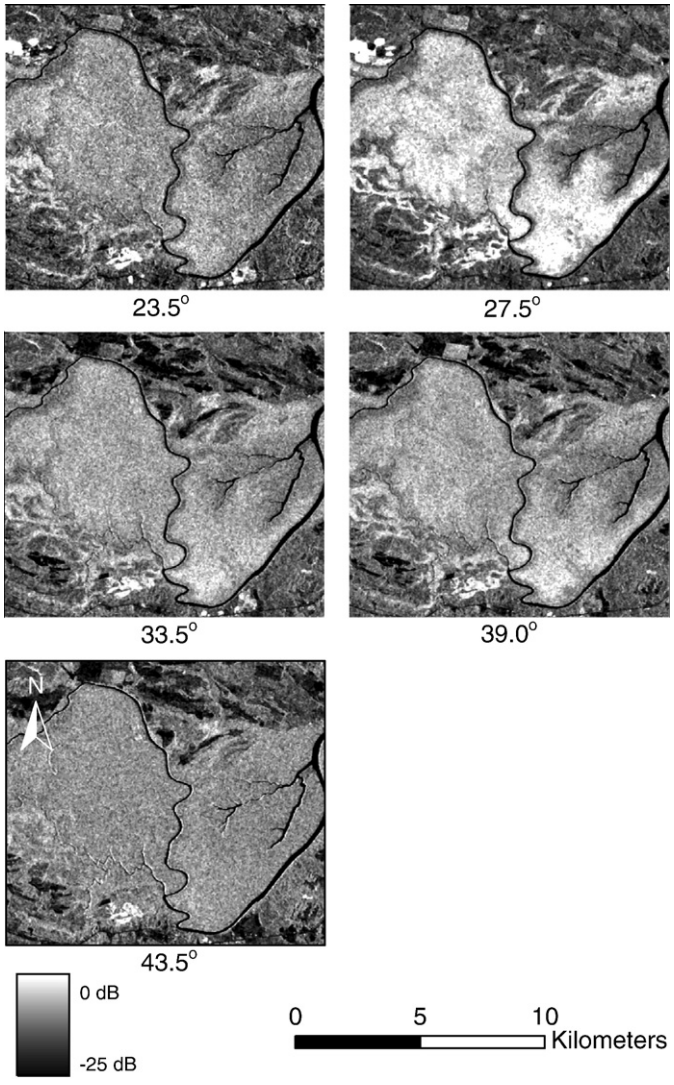

Fig. 4. A small portion of the leaf-on Radarsat-1 images in order of increasing incidence angle. All images are from May or June 2000, and were collected during a period of similar river discharge. Please see Fig. 2 for the location of this sample area relative to the entire study site. Pixel values ranged from 0 dB (white) to −25 dB (black).

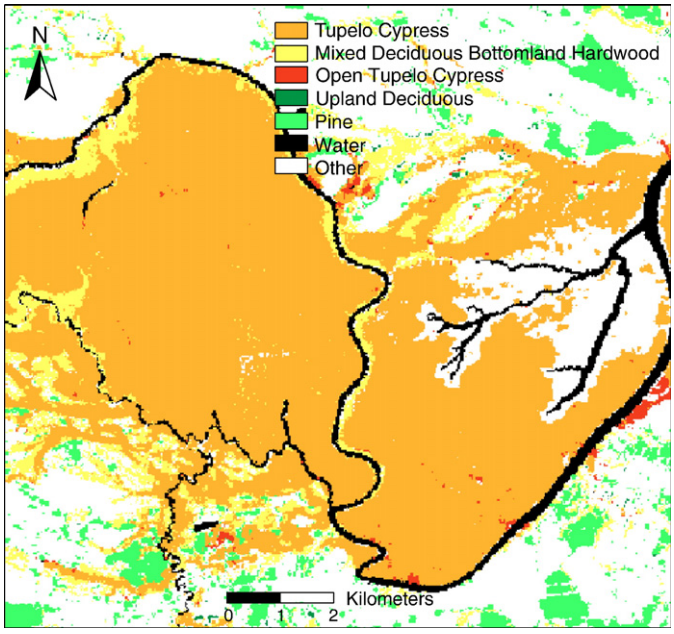

Fig. 5. A sample of the forest classification map used to identify forest types showing the same area as illustrated in Figs. 3 and 4. Tupelo-cypress forests compose the majority of floodplain forests while mixed deciduous bottomland hardwood forests are located in linear patches along the river or in other areas of slightly higher elevation mainly within the floodplain. Pine forests are mainly located in large but discrete patches further from the river. Upland deciduous and open tupelo-cypress forests are found in much smaller patches relative to the other forest types. Please note that the area exhibited in this illustration represents a small portion of the entire study site.

ground control points from a Landsat Thematic Mapper (TM) image. The cumulative root mean square error was <15 m and a second order polynomial transformation and nearest neighbor resampling were used for georeferencing. Calibration data provided by the Alaska Satellite Facility were used to convert radar intensity data to backscatter coefficients.

To isolate effects of physiognomic differences among forests, the analyses were stratified by five forest types: Open tupelo-cypress, tupelo-cypress, mixed deciduous bottomland hardwood, upland deciduous, and pine. Forest types were identified using a digital vegetation classification derived from Landsat TM and ground data (Townsend & Walsh, 2001). Tupelo-cypress forests were separated from other types of floodplain forest because they are structurally distinct. On average, tupelo-cypress forests had a higher basal area (>50 m^2/ha), fewer small trees, and increased trunk buttressing as compared to mixed deciduous bottomland hardwood forests (Townsend 2002). These variations may enhance double-bounce scattering of microwave energy. Other forest types were separated due to more obvious differences, such as the decreased canopy closure and basal area of open tupelo-cypress forests compared to tupelo-cypress forests and the varying structure and leaf type of pine forests.

Forest patches were identified using the vegetation classification. Only interior areas of the five forest types were evaluated to decrease the chance of mixing or incorrectly identifying forest types. Interior areas were defined as those pixels 60 m or more from an edge with a different cover type for tupelo-cypress, bottomland hardwood and pine forests, and 30 m or more for less extensive open tupelo-cypress and upland deciduous forests.

Flood extent was estimated for all eleven Radarsat-1 images using a digital elevation and river discharge based flood simulation model as well as thresholds of SAR backscatter coefficient (Townsend, 2001; Townsend & Foster, 2002). Flooded and non-flooded areas were verified with both the model and the SAR backscatter coefficient thresholds for each date, and were only used when there was agreement between both sources.

Average backscatter coefficient was assessed for flooded and non-flooded areas in open tupelo-cypress, tupelo-cypress, and mixed deciduous bottomland hardwood forests while average backscatter coefficient was assessed in non-flooded areas for upland deciduous and pine forests. Standard deviation in dB was calculated for each backscatter coefficient sample (Kasischke & Fowler, 1989).

Table 1
Dates, incidence angles, stream discharge, average 2 day precipitation, and season for Radarsat-1 acquisitions

Date	Incidence angle range	Average	Discharge (cm)	Precip (cm)	Season
12/2/2000	41°–46°	43.5°	58	0.00	Leaf-off
12/6/2000	20°–27°	23.5°	107	0.00	Leaf-off
12/9/2000	36°–42°	39.0°	169	0.00	Leaf-off
12/16/2000	30°–37°	33.5°	59	0.12	Leaf-off
12/19/2000	45°–49°	47.0°	86	0.00	Leaf-off
12/23/2000	24°–31°	27.5°	57	0.00	Leaf-off
5/21/2000	24°–31°	27.5°	113	1.17	leaf-on
5/31/2000	36°–42°	39.0°	136	1.04	leaf-on
6/7/2000	30°–37°	33.5°	170	0.51	leaf-on
6/17/2000	41°–46°	43.5°	97	0.53	leaf-on
6/21/2000	20°–27°	23.5°	256	3.58	leaf-on

Table 2
Average incidence angle per date for each forest type and flood condition (flooded or non-flooded [NF])

	Bottomland		Tupelo-cypress		Opn Tupelo-Cypress		Upl Dec	Pine
	Flood	NF	Flood	NF	Flood	NF	NF	NF
12/2/2000	43.75	43.40	44.09	44.02	43.70	43.52	42.52	44.19
12/6/2000	22.50	21.99	22.89	22.83	22.35	22.12	21.16	23.08
12/9/2000	39.52	39.06	39.82	39.72	39.37	39.18	38.10	39.92
12/16/2000	33.63	33.19	34.04	33.96	33.56	33.33	32.13	34.17
12/19/2000	48.66	48.21	48.74	48.74	48.50	48.29	47.39	48.75
12/23/2000	28.64	28.06	29.03	28.73	28.40	28.23	26.91	29.08
5/21/2000	28.24	27.76	28.66	28.34	28.12	27.91	26.60	28.68
5/31/2000	39.68	39.12	39.88	39.75	39.40	39.27	38.17	39.98
6/7/2000	33.65	33.11	33.91	33.65	33.39	33.25	32.06	34.09
6/17/2000	43.90	43.49	43.96	43.90	43.74	43.60	42.61	44.27
6/21/2000	23.77	22.13	22.99	22.46	22.43	22.23	21.32	23.24

The forest types included in the graph are: bottomland hardwood (Bottomland), tupelo-cypress, open tupelo-cypress (Opn Tupelo-Cypress), upland deciduous (Upl Dec), and pine.

4. Results

Average incidence angle for all forest types and flood conditions (i.e., flooded or non-flooded) per date was found to be similar to the

Table 3
Sample size (number of pixels) in each forest type under flooded and non-flooded (NF) conditions during each Radarsat-1 acquisition

	Bottomland		Tupelo-cypress		Opn tupelo-cypress		Upl Dec	Pine
	Flood	NF	Flood	NF	Flood	NF	NF	NF
12/2/2000	51	69,660	44,742	95,731	1263	1688	1503	470,185
12/6/2000	61	69,650	35,717	104,756	1244	1707	1503	470,185
12/9/2000	66	69,645	45,834	94,639	1280	1671	1503	470,185
12/16/2000	49	69,662	42,154	98,319	1267	1684	1503	470,185
12/19/2000	30	69,681	23,443	117,030	1130	1821	1503	470,185
12/23/2000	101	69,610	79,691	60,782	1561	1390	1503	470,185
5/21/2000	53	69,658	72,483	67,990	1195	1756	1503	470,185
5/31/2000	69	69,642	44,255	96,218	1346	1605	1503	470,185
6/7/2000	135	69,576	63,317	77,156	1580	1371	1503	470,185
6/17/2000	137	69,574	32,060	108,413	1666	1285	1503	470,185
6/21/2000	107	69,604	58,454	82,019	1664	1287	1503	470,185

The forest types included in the graph are: Bottomland hardwood (Bottomland), tupelo-cypress, open tupelo-cypress (Opn Tupelo-Cypress), upland deciduous (Upl Dec), and pine.

Table 4
Standard deviation, in dB (Kasischke and Fowler 1989), for all forest types during each Radarsat-1 acquisition

	Bottomland		Tupelo-cypress		Opn tupelo-cypress		Upl Dec	Pine
	Flood	NF	Flood	NF	Flood	NF	NF	NF
12/2/2000	0.468	0.423	0.387	0.410	0.369	0.518	1.054	0.660
12/6/2000	0.522	0.817	0.148	0.297	0.272	0.787	1.232	0.758
12/9/2000	0.444	0.698	0.250	0.457	0.287	0.757	1.171	0.710
12/16/2000	0.303	0.664	0.205	0.398	0.260	0.654	1.271	0.733
12/19/2000	0.511	0.572	0.652	0.816	0.433	0.856	0.943	1.348
12/23/2000	0.240	1.213	0.336	0.520	0.355	0.829	0.956	0.829
5/21/2000	1.146	0.592	0.645	0.595	0.702	0.725	0.610	2.705
5/31/2000	0.412	0.413	0.321	0.349	0.377	0.481	0.450	0.661
6/7/2000	0.356	0.421	0.305	0.341	0.346	0.459	1.841	0.579
6/17/2000	0.599	0.418	0.336	0.345	0.509	0.473	1.212	0.511
6/21/2000	0.670	0.480	0.339	0.342	0.378	0.513	2.249	0.853

average incidence angle for the entire image (Table 2). Under non-flooded conditions, >1000 samples (pixels) of SAR backscatter coefficient were identified for all forest types (Table 3). Under flooded conditions, >1000 samples (pixels) of SAR backscatter coefficient were extracted for all forest types except for bottomland hardwood. Although bottomland hardwood areas had the smallest sample size, the standard deviation of these measurements was similar to that of the other wetland forest types (Table 4). Under non-flooded conditions, tupelo-cypress forests had the highest backscatter coefficient values, with a relatively large increase (>3 dB) in backscatter coefficient during the leaf-off season compared to the leaf-on season (Fig. 6). Non-flooded bottomland hardwood and upland deciduous forests behaved similarly across all incidence angles, with bottomland hardwood forests having slightly higher average backscatter coefficient (0.3 dB greater leaf-on and 0.4 dB greater leaf-off) at all times and incidence angles. Average backscatter coefficient from pine forests was slightly higher (0.6 dB higher) during the leaf-on season than leaf-off at all incidence angles except 33.5°. A general, subtle trend of decreasing backscatter with increasing incidence angle was more evident during the leaf-off period than leaf-on. However, it should be noted that there were exceptions to this subtle trend in decreasing backscatter and slope was not constant between incidence angles. For example, during the leaf-on period, backscatter coefficient at 23.5° decreased by about 3 dB for all flooded forests compared to the leaf-off period (Fig. 6).

During the leaf-off period, the ability to detect flooding was fairly constant for both types of tupelo-cypress forest, although flooding yielded greater differences in backscatter coefficient in open tupelo-cypress forests than tupelo-cypress forests (Fig. 7). Bottomland hardwood forests had about a 2 dB greater difference in backscatter between flooded and non-flooded areas than open tupelo-cypress forests, with data collected at 27.5° having the greatest difference and data collected at 23.5° and 47.0° having the least difference.

The ability to detect flooding during leaf-on conditions varied much more according to incidence angle while forest type had a greater effect during the leaf-off season (Fig. 7). Generally, across all forest types, an incidence angle of 23.5° provided the smallest difference in backscatter coefficient between flooded and non-flooded forests while the incidence angle that provided the largest difference in backscatter coefficient between flooded and non-flooded conditions varied with forest type. Past research indicated that the difference in backscatter coefficient between flooded and non-flooded conditions would be larger during the leaf-off season (Kasischke et al., 1997; Townsend, 2001; Townsend & Foster, 2002), but this was not always the case (Fig. 7). Specifically, tupelo-cypress forests exhibited a greater difference in backscatter between flooded and non-flooded areas during the leaf-on as compared to the leaf-off season.

Backscatter coefficient from all of the floodplain forest types was averaged to illustrate general trends, regardless of forest type. This analysis is necessary to illustrate general trends in the relationship between backscatter, incidence angle and flooding because forest type data may not always be available for operational studies (e.g., natural disaster assistance). Backscatter was found to generally decrease

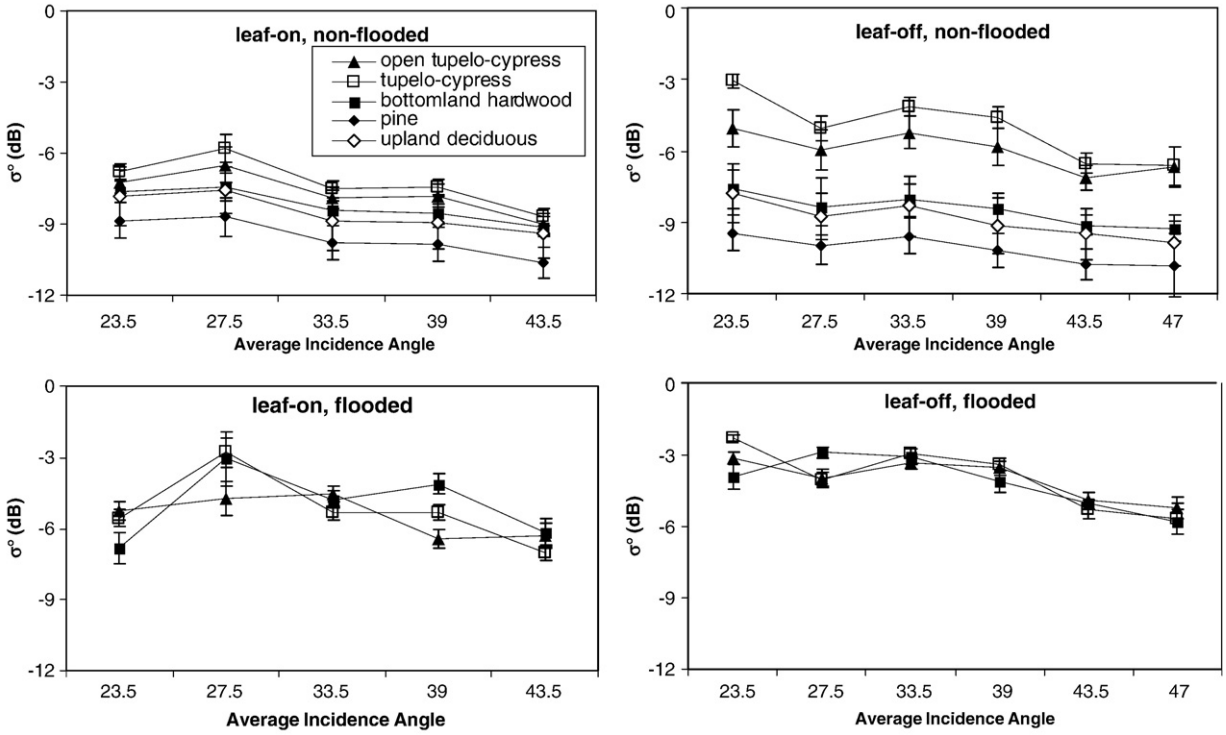

Fig. 6. Backscatter coefficient (σ°) and standard deviations as a function of average image incidence angle for all forest types during leaf-on, non-flooded (top left), leaf-off, non-flooded (top right), leaf-on, flooded (bottom left), and leaf-off, flooded (bottom right) conditions. Please note that incidence angle for each data point viewed above varies slightly with forest type and flood condition (i.e., flooded or non-flooded; Table 2). Standard deviations exhibited in this figure can be found in Table 4.

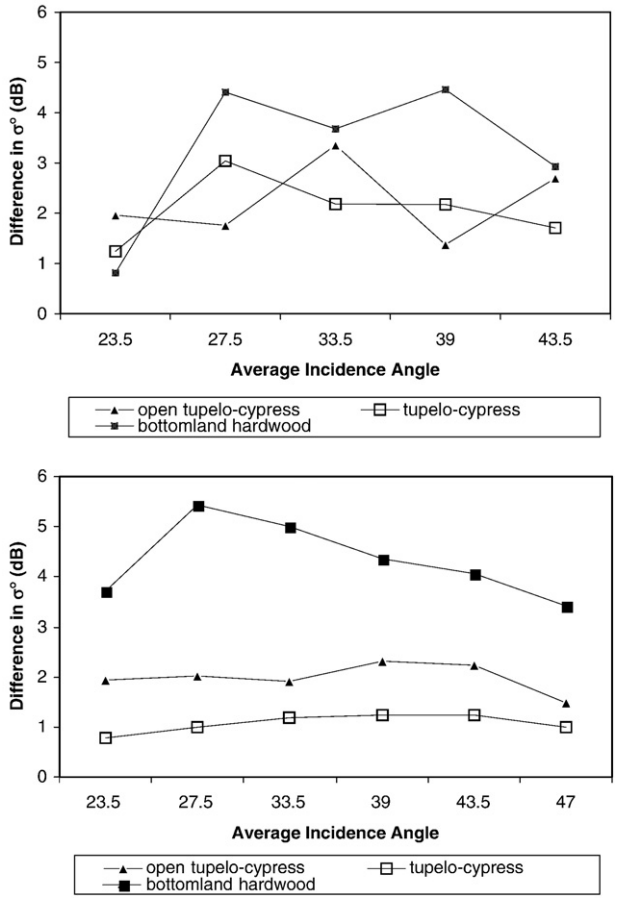

Fig. 7. Difference in backscatter coefficient (σ°) between flooded and non-flooded forests for all floodplain forest types as a function of average image incidence angle during the leaf-on (top) and leaf-off (bottom) seasons. Please note that incidence angle for each data point viewed above varies slightly with forest type and flood condition (i.e., flooded or non-flooded; Table 2).

(although the trend is not absolute) with increasing incidence angle under all conditions (2.45 dB between 23.5° and 47.0° flooded, leaf-off; 2.28 dB between 23.5° and 47.0° not flooded, leaf-off; 0.62 between 23.5° and 43.5° flooded, leaf-on; 1.73 dB between 23.5° and 43.5° not flooded, leaf-on; Fig. 8). However, the distinction between

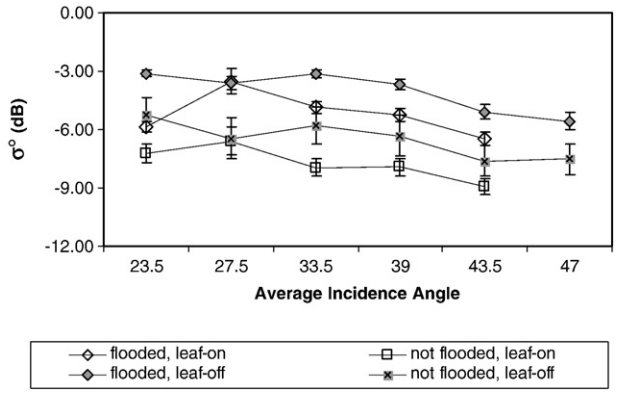

Fig. 8. Backscatter coefficient (σ°; averaged for all floodplain forest types) and standard deviations as a function of average image incidence angle during the leaf-on and leaf-off seasons, under flooded and non-flooded conditions. Incidence angle for each data point viewed above varies slightly with forest type and flood condition (i.e., flooded or non-flooded; Table 2). Please note that average trends for all forest types are represented above and that response from individual forests vary (Fig. 6).

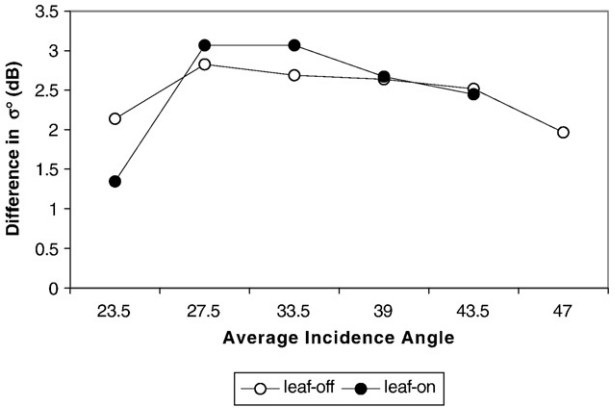

Fig. 9. Difference in backscatter coefficient (σ°) between flooded and non-flooded areas as a function of incidence angle. Values are an average of all floodplain forest types. Incidence angle for each data point viewed above varies slightly with forest type and flood condition (i.e., flooded or non-flooded; Table 2). Please note that response from individual forests vary (Fig. 7).

flooded and non-flooded areas did not decline sharply with incidence angle, as expected (Fig. 9). Although previous research (Bourgeau-Chavez et al., 2001; Ford & Casey, 1988; Hess et al., 1990; Richards et al., 1987; Töyrä et al., 2001; Wang et al., 1995) has often supported the use of smaller incidence angles to detect inundation in forests, data collected at the 23.5° incidence angle exhibited one of, if not the smallest difference between flooded and non-flooded forests. Conversely, the ability to detect inundation under flooded forests was greater than expected at larger incidence angles (Fig. 9; Bourgeau-Chavez et al., 2001; Ford & Casey, 1988; Richards et al., 1987; Töyrä et al., 2001; Wang et al., 1995). The ability to differentiate flooded and non-flooded forests was similar during the leaf-off and leaf-on seasons (Fig. 9).

5. Discussion

Previous research has indicated that flooding should be more detectable in forests using radar data collected at smaller (steeper) incidence angles (Bourgeau-Chavez et al., 2001; Ford & Casey, 1988; Richards et al., 1987; Töyrä et al., 2001; Wang et al., 1995). This research suggests that this may not always be the case (Figs. 7 and 9). It was hypothesized that larger incidence angle data would encounter decreased transmissivity in the canopy layer and therefore be less sensitive to flooding on the ground. This decrease in transmissivity may have led to a general, subtle decline in total backscatter with increasing incidence angle, but it did not lead to a substantial decrease in sensitivity to flooding as found by previous studies (Ford & Casey, 1988; Töyrä et al., 2001; Wang et al., 1995). In fact, C-HH SAR data collected at the smallest incidence angle considered by this study (average incidence angle 23.5°) exhibited very close to, if not the smallest average difference in backscatter coefficient between flooded and non-flooded areas.

The comparatively low ability of Radarsat-1 SAR data collected at 23.5° to distinguish between flooded and non-flooded areas occurs during both the leaf-on and leaf-off periods (Fig. 9). This may result from the orientation of canopy leaves during the leaf-on season. For all of the major floodplain tree species (except the coniferous cypress), leaf length is about the same or longer than the microwave wavelength (5.6 cm), and leaf orientation can be assumed to be uniform to normal. Therefore, energy transmitted at the smallest incidence angle (23.5°) was more likely to encounter the front of leaves (the largest surface area of the leaf), while energy at larger incidence angles was more likely to encounter the narrow leaf sides and pass through the canopy via gaps between leaves. The decreased ability of data collected at 23.5° to detect flooding in bottomland

hardwood forests during the leaf-off and leaf-on seasons (Fig. 7) may have to do with the presence of ground cover, which is absent from the tupelo-cypress and open tupelo-cypress forests. The largest incidence angle data, 47°, was only available during the leaf-off period. It also exhibited a level of sensitivity similar to the smallest incidence angle data examined.

Although data collected at average incidence angles of 27.5° and 33.5° were found to provide the best discrimination between flooded and non-flooded forests (Fig. 9), this study demonstrated that shallower incidence angles could also be used to accurately distinguish flooded from non-flooded forests. All of the larger incidence angles exhibited a difference in backscatter >1 dB, which surpasses the relative calibration error for Radarsat-1 (Srivastava et al., 1993).

Although the ability of C-band SAR to detect flooding is generally expected to decrease substantially in forests during the leaf-on season (Wang et al., 1995), our results support other studies (Townsend & Walsh, 1998; Townsend, 2001), which concluded that flooding could be detected in forests during leaf-off and leaf-on seasons (Fig. 9). In fact, flooding was found to be slightly easier to detect during the leaf-on season at moderate incidence angles (average incidence angles of 27.5° and 33.5°), but this small (<0.5 dB) difference is not likely to be significant. Flooding was easier to detect during the leaf-off season at smaller incidence angles, while the presence of leaves had no impact at average incidence angles of 39° and 43.5°.

The angular signatures of non-flooded tupelo-cypress and open tupelo-cypress forests were more distinct than other forest types during the leaf-off season (Fig. 6). At this time of year, backscatter from the tupelo-cypress forest types was about 2.5 dB greater than the other forests, while during the leaf-on season it was only about 0.6 dB higher. This result may be a consequence of higher transmissivity through the canopy layer during the leaf-off season, leading to greater sensitivity to the higher soil moisture levels (and therefore greater backscatter) characteristic of tupelo-cypress forests. Townsend (2002) also found distinctions between forest types to be influenced by environmental conditions, and Wang et al. (1998) and Lang and Kasischke (2008) noted that surface characteristics, like soil moisture, influence backscatter from forests. This likely difference in soil moisture may also explain the slightly higher backscatter from the non-flooded bottomland hardwood forests compared to the upland deciduous forests. It is notable that pine forests, which are generally found in drier areas than deciduous forests, exhibited the lowest backscatter. However, this can only be attributed to lower soil moisture if transmission in the canopy and trunk layers was sufficient (i.e., extinction coefficient was sufficiently low based on biomass of the pine trees; Dobson et al., 1995). Precipitation does not appear to have had a significant effect on the angular signature. Although precipitation did occur before overpasses, it did so in a relatively consistent manner (Table 1). All leaf-on images had rain within two days of overpass and all leaf-off images had very little or no rain within two days of the overpass. Backscatter response on December 16, 2000 (average incidence angle of 33.5°), the only leaf-off day with rain (.12 cm) within two days of overpass, did not increase notably as would be expected if rain significantly increased soil moisture (Fig. 6). Other factors that could potentially impact the angular signature of the different forest types include subtle variations in flood depth and differences in the exact location of flooding during image collection dates. The potential impact of these factors has been reduced by selecting a study site with relatively flat topography, imagery dates with limited variations in flood depth, and grouping forests according to structural variations between forests and other biophysical characteristics.

Under non-flooded conditions during the leaf-off season, the angular signatures of open tupelo-cypress and tupelo-cypress converged at larger incidence angles (Fig. 6). This may reflect the lower sensitivity of the microwave signal to soil moisture at larger incidence angles reported by Dobson et al. (1983). As expected, the potential impact of soil moisture on backscatter values is reduced during the leaf-on season (increased attenuation of the forest canopy) as supported by smaller differences in average backscatter between forest types.

The angular backscatter signatures were least consistent among forest types under flooded conditions during the leaf-on period (Fig. 6). These differences in backscatter coefficients between forest types may have resulted from physiognomic variations in the canopy, and the resulting differences in backscatter response that occur as a consequence of double-bounce and multi-path scattering in flooded forests. This assertion is supported by the distinction in angular signatures between the open and closed canopy tupelo-cypress forests and the greater similarity between the angular signatures of the closed canopy tupelo-cypress and the bottomland deciduous forests (also closed canopy). This occurred even though closed canopy tupelo-cypress forests are characterized by buttressed trunks and therefore greater basal area than bottomland hardwood forests. The increasing impact of forest characteristics on backscatter with the addition of inundation was also reported by Townsend (2002) who suggests that this may be due to a decrease in the impact of ground surface characteristics caused by flooding and/or the increase in interactions with the trunk and crown layer due to double-bounce and multi-path scattering.

In flooded leaf-off forests, backscatter exhibited a clear trend of decreasing backscatter with increasing incidence angle that was not obvious in the flooded, leaf-on data (Fig. 6). Specular reflectance lowers backscatter at higher incidence angles, but this impact is lessened when the presence of the canopy re-directs specular reflectance back towards the sensor. Increasing specular reflectance with decreasing canopy closure was reported by Rauste (1990). This trend is especially evident because the impact of the varying character of the ground layer between forest types is eliminated by the presence of standing water.

The incidence angle that was most sensitive to flooding varied according to forest type. However, the difference in angular signatures between flooded and non-flooded forests was much more consistent across incidence angles during the leaf-off season (Fig. 7). The increasing variation in backscatter with changes in incidence angle during the leaf-on season could have resulted from greater interaction of the radar signal with the trunk and canopy layers caused by the increase in canopy closure during the leaf-on season (Townsend, 2002). This increased interaction may encourage the differentiation of forest types that vary not only in canopy closure but also in basal area and trunk shape. The greater ability to distinguish flooding in the deciduous bottomland forests may result from the generally lower soil moisture found at these sites (compared to tupelo-cypress) when they are not inundated. As a general rule, the difference in backscatter response between forests with drier soil and inundated forests is greater than the difference in backscatter between forests with wet soils and inundated forests.

6. Summary and conclusions

Backscatter from Radarsat-1 C-HH SAR data varied as a function of incidence angle, as well as vegetation structure, flooding, and possibly soil moisture. A simple model of radar cumulative backscatter response from forested wetlands (Eq. (1)) relates changes in total backscatter coefficient to *in situ* conditions. The following describes the hypothesized influences of *in situ* conditions on the parameters found in Eq. (1). Specifically, we found a subtle trend of generally decreasing backscatter with increasing incidence angle. We hypothesize that this decrease was caused by lower transmissivity of the crown layer (τ_c), increased attenuation of energy from double-bounce (σ°_d) and multi-path (σ°_m) scattering, and possibly increased specular reflectance of the surface layer (σ°_s) with increasing incidence angle.

In the absence of flooding, differences in soil moisture distinguished the different forest types. Forests that normally have nearly

saturated soils (tupelo-cypress) had a higher surface layer backscatter coefficient (σ°_{s}), and therefore greater total backscatter than forests with drier soils. Forests that normally have lower soil moisture (upland deciduous and pine) had a lower surface layer backscatter coefficient (σ°_{s}) and consequently lower total backscatter. This difference was more apparent during the leaf-off season, when the transmissivity of the crown layer (τ_c) was highest, allowing more energy to penetrate the canopy layer and interact with the surface layer. The ability to distinguish differences in soil moisture (inferred by forest type) decreased slightly with increasing incidence angle with the sharpest declines at incidence angles greater than or equal to 47°.

Under flooded conditions, variations between the surface layers of forest types were minimized and double-bounce (σ°_{d}) and multi-path (σ°_{m}) backscatter increased at all incidence angles, although most noticeably at 27.5° and 33.5°. When flooded during the leaf-on season, canopy variations among the different forest types were accentuated by increased multi-path (σ°_{m}) and double-bounce (σ°_{d}) scattering which, in turn, increased canopy scattering (σ°_{c}) and decreased net surface scattering (σ°_{s}). The variation in total backscatter due to differences in canopy closure was most obvious at incidence angles of 27.5° and 39°. During the leaf-off period, variations in canopy closure were minimized due to the overall increase in canopy transmissivity (τ_c).

Overall, flooding was easier to detect in the bottomland hardwood forests compared to other forest types. However, the ability to detect flooding varied more with incidence angle during the leaf-on period and more with forest type during the leaf-off period. During the leaf-on period, canopy transmissivity (τ_c) was primarily responsible for variation in the ability to detect flooding with increasing incidence angle. Our data suggest that during the leaf-off period, the surface backscatter coefficient (σ°_{s}) (e.g., different levels of soil moisture) was more influential. The relatively large drop in the ability of the smallest incidence angle (23.5°) to detect flooding may have been due to the orientation of canopy leaves parallel to the surface layer. This orientation may decrease canopy transmissivity (τ_c) at steep (small) incidence angles.

Our results indicate that a wide variety of incidence angles and times of the year can be used when monitoring inundation under forest canopies using C-HH band SAR data, which may facilitate monitoring of highly dynamic flood events. Satellite resources could be rapidly redeployed, given the wider range of acceptable incidence angles, to image flooding brought on by natural disasters and human actions, such as dam releases, regardless of season. This has the potential to benefit a variety of natural resource management issues. For example, although monthly monitoring of wetland hydropattern is able to capture the general pattern of flooding in wetlands, higher temporal resolution could better measure the period of flooding needed to form commonly used indicators of wetland presence, such as hydric soils and hydrophytic vegetation. Although scientists agree that prolonged saturation of the upper substrate is necessary for the formation of wetlands, further research is needed to more precisely identify the threshold duration of saturation required for wetland creation (National Research Council, 1995). In addition to wetland delineation, the characterization of "normal" or average hydropattern could help to guide the management of existing and the establishment of new wetlands, since maintenance of a natural hydropattern is vital.

The results of this research suggest the need for further examination of multiple incidence angle SAR data elsewhere, especially in other forest types. This is particularly important since some studies have demonstrated that the increase in backscatter when forests are flooded does not always occur, possibly due to very dense canopies and undergrowth (reduced transmission) or short, small diameter trees (reduced surface for double-bounce; Hess et al., 1990). Additional wavelengths and polarizations of SAR data should also be explored. The analysis of other wavelengths will increase the understanding of scattering and attenuation mechanisms from structures of varying sizes (e.g. leaves, trunks, and branches) while the evaluation of other polarizations will increase the understanding of scattering and attenuation mechanisms due to the spatial orientation of these structures.

Acknowledgements

This research was conducted while the lead author was a graduate student at the University of Maryland and the second author was on the faculty of the University of Maryland Center for Environmental Science — Appalachian Laboratory. This work was supported by a NASA Earth System Science Fellowship, the Application Development and Research Opportunity (ADRO) program, and The Nature Conservancy. The research facility was provided by the Mid-Atlantic Regional Earth Science Applications Center and the University of Maryland, Department of Geography. The authors wish to thank Jane Foster and Clayton Kingdon for assistance with data processing. Finally, we wish to thank the editor and two anonymous reviewers for their helpful comments and suggestions.

References

Bourgeau-Chavez, L. L., Kasischke, E. S., Brunzell, S. M., Mudd, J. P., Smith, K. B., & Frick, A. L. (2001). Analysis of space-borne SAR data for wetland mapping in Virginia riparian ecosystems. *International Journal of Remote Sensing*, *22*, 3665–3687.

Bourgeau-Chavez, L. L., Smith, K. B., Brunzell, S. M., Kasischke, E. S., Romanowicz, E. A., & Richardson, C. J. (2005). Remote sensing of regional inundation patterns and hydroperiod in the greater Everglades using synthetic aperture radar. *Wetlands*, *25*, 176–191.

Conly, F. M., & Van der Kamp, G. (2001). Monitoring the hydrology of Canadian prairie wetlands to detect the effects of climate change and land use changes. *Environmental Monitoring and Assessment*, *67*, 195–215.

Costa, M. P. F. (2004). Use of SAR satellites for mapping zonation of vegetation communities in the Amazon floodplain. *International Journal of Remote Sensing*, *25*, 1817–1835.

Dobson, M. C., Ulaby, F. T., Moezzi, S., & Roth, E. (1983). A simulation study of the effects of land cover and crop type on sensing soil moisture with an orbital c-band radar. *IEEE International Geosciences and Remote Sensing Symposium (IGARSS '83), San Francisco, C.A.*

Dobson, M. C., Ulaby, F. T., Pierce, L. E., Sharik, T. L., Bergen, K. M., Kellndorfer, J., et al. (1995). Estimation of forest biophysical characteristics in Northern Michigan with SIR-C/X-S. *IEEE Transactions on Geoscience and Remote Sensing*, *33*, 877–895.

Engheta, N., & Elachi, C. (1982). Radar scattering from a diffuse vegetation layer over a smooth surface. *IEEE Transactions on Geoscience and Remote Sensing*, *20*, 212–216.

Engman, E. T. (1996). Remote sensing applications to hydrology: Future impact. *Hydrological Sciences Journal*, *41*, 637–647.

Ford, J. P., & Casey, D. J. (1988). Shuttle radar mapping with diverse incidence angles in the rainforest of Borneo. *International Journal of Remote Sensing*, *9*, 927–943.

Hall, D. K. (1996). Remote sensing applications to hydrology: Imaging radar. *Hydrological Sciences Journal*, *41*, 609–624.

Hess, L. L., Melack, J. M., Filoso, S., & Wang, Y. (1995). Delineation of inundated area and vegetation along the Amazon floodplain with the SIR-C synthetic aperture radar. *IEEE Transactions on Geoscience and Remote Sensing*, *33*, 896–904.

Hess, L. L., Melack, J. M., & Simonett, D. S. (1990). Radar detection of flooding beneath the forest canopy: A review. *International Journal of Remote Sensing*, *11*, 1313–1325.

Imhoff, M., Story, M., Vermillion, C., Khan, F., & Polcyn, F. (1986). Forest canopy characterization and vegetation penetration assessment with space-borne radar. *IEEE Transactions on Geoscience and Remote Sensing*, *24*, 535–542.

Imhoff, M. L., Vermillion, C., Story, M. H., Choudhury, A. M., Gafoor, A., & Polcyn, F. (1987). Monsoon flood boundary delineation and damage assessment using space borne imaging radar and Landsat data. *Photogrammetric Engineering and Remote Sensing*, *53*, 405–413.

Kandus, P., Karszenbaum, H., Pultz, T., Parmuchi, G., & Bava, J. (2001). Influence of flood conditions and vegetation status on the radar backscatter of wetland ecosystems. *Canadian Journal of Remote Sensing*, *27*, 651–662.

Kasischke, E. S., & Bourgeau-Chavez, L. L. (1997). Monitoring south Florida wetlands using ERS-1 SAR imagery. *Photogrammetric Engineering and Remote Sensing*, *63*, 281–291.

Kasischke, E. S., & Fowler, G. W. (1989). A statistical approach for determining radiometric precision and accuracies in the calibration of synthetic aperture radar imagery. *IEEE Transactions on Geoscience and Remote Sensing*, *27*, 416–427.

Kasischke, E. S., Melack, J. M., & Dobson, M. C. (1997). The use of imaging radars for ecological applications — A review. *Remote Sensing of Environment*, *59*, 141–156.

Kasischke, E. S., Smith, K. B., Bourgeau-Chavez, L. L., Romanowicz, E. A., Brunzell, S., & Richardson, C. J. (2003). Effects of seasonal hydrologic patterns in south Florida wetlands on radar backscatter measured from ERS-2 SAR imagery. *Remote Sensing of Environment*, *88*, 423–441.

Krohn, M. D., Milton, N. M., & Segal, D. B. (1983). Seasat synthetic aperture radar (SAR) response to lowland vegetation types in eastern Maryland and Virginia. *Journal of Geophysical Research-Oceans and Atmospheres*, *88*, 1937–1952.

Lang, M. W., & Kasischke, E. S. (2008). Using Synthetic aperture radar data to monitor forested wetland hydrology in Maryland's Coastal Plain, USA. *IEEE Transactions on Geoscience and Remote Sensing*, *46*, 535–546.

Magagi, R., Bernier, M., & Ung, C. H. (2002). Quantitative analysis of RADARSAT SAR data over a sparse forest canopy. *IEEE Transactions on Geoscience and Remote Sensing*, *40*, 1301–1313.
McDonald, K. C., Dobson, M. C., & Ulaby, F. T. (1990). Using MIMICS to model L-band multiangle and multitemporal backscatter from a walnut orchard. *IEEE Transactions on Geoscience and Remote Sensing*, *28*, 47–491.
Mendoza, G. F., Steenhuis, T. S., Walter, M. T., & Parlange, J. Y. (2003). Estimating basin-wide hydraulic parameters of a semi-arid mountainous watershed by recession-flow analysis. *Journal of Hydrology*, *279*, 57–69.
Mitsch, W. J., & Gosselink, J. G. (2000). *Wetlands.* New York: John Wiley & Sons, Inc.
National Research Council (1995). *Wetlands: Characteristics and Boundaries.* Washington: National Academy Press.
Ormsby, J. P., Blanchard, B. J., & Blanchard, A. J. (1985). Detection of lowland flooding using active microwave systems. *Photogrammetric Engineering and Remote Sensing*, *51*, 317–328.
Place, J. L. (1985). Mapping of forested wetland: Use of Seasat radar images to complement conventional sources. *Professional Geographer*, *37*, 463–469.
Pope, K. O., Rejmankova, E., Paris, J. F., & Woodruff, R. (1997). Detecting seasonal flooding cycles in marshes of the Yucatan Peninsula with SIR-C polarimetric radar imagery. *Remote Sensing of Environment*, *59*, 157–166.
Price, J. S., Branfireun, B. A., Waddington, J. M., & Devito, K. J. (2005). Advances in Canadian wetland hydrology, 1999–2003. *Hydrological Processes*, *19*, 201–214.
Rao, B. R. M., Dwivedi, R. S., Kushwaha, S. P. S., Bhattacharya, S. N., Anand, J. B., & Dasgupta, S. (1999). Monitoring the spatial extent of coastal wetlands using ERS-1 SAR data. *International Journal of Remote Sensing*, *20*, 2509–2517.
Rauste, Y. (1990). Incidence-angle dependence in forested and non-forested areas in Seasat SAR data. *International Journal of Remote Sensing*, *11*, 1267–1276.
Richards, J., Sun, G. Q., & Simonett, D. (1987). L-band radar backscatter modeling of forest stands. *IEEE Transactions on Geoscience and Remote Sensing*, *25*, 487–498.
Srivastava, S. K., Le Dantec, P., Hawkins, R. K., Banik, B. T., Gray, R., Murnaghan, K., et al. (1993). RADARSAT-1 image quality and calibration — Continuing success in extended mission. *Advances in Space Research*, *32*, 2295–2304.
Sun, G., & Simonett, D. (1988). Simulation of L-band HH microwave backscattering from coniferous forest stands: a comparison with SIR-B data. *International Journal of Remote Sensing*, *9*, 907–925.
Tiner, R. (1999). *Wetland Indicators: A Guide to Wetland Identification, Delineation, Classification, and Mapping.* Washington: Lewis Publishers.
Townsend, P. A. (2000). A quantitative fuzzy approach to assess mapped vegetation classifications for ecological applications. *Remote Sensing of Environment*, *72*, 253–267.
Townsend, P. A. (2001). Mapping seasonal flooding in forested wetlands using multi-temporal radarsat SAR. *Photogrammetric Engineering and Remote Sensing*, *67*, 857–864.
Townsend, P. A. (2002). Relationships between forest structure and the detection of flood inundation in forested wetlands using C-band SAR. *International Journal of Remote Sensing*, *23*, 443–460.
Townsend, P. A., & Foster, J. R. (2002). A synthetic aperture radar-based model to assess historical changes in lowland floodplain hydroperiod. *Water Resources Research*, *38*, 1115.
Townsend, P. A., & Walsh, S. J. (1998). Modeling floodplain inundation using an integrated GIS with radar and optical remote sensing. *Geomorphology*, *21*, 295–312.
Townsend, P. A., & Walsh, S. J. (2001). Remote sensing of forested wetlands: Application of multitemporal and multispectral satellite imagery to determine plant community composition and structure in southeastern USA. *Plant Ecology*, *157*, 129–149.
Töyrä, J., Pietronira, A., & Martz, L. (2001). Multisensor hydrologic assessment of a freshwater wetland. *Remote Sensing of Environment*, *75*, 162–173.
Wang, Y., Day, J. L., & Davis, F. W. (1998). Sensitivity of modeled C- and L-band radar backscatter to ground surface parameters in loblolly pine forest. *Remote Sensing of Environment*, *66*, 331–342.
Wang, Y., Hess, L. L., Filoso, S., & Melack, J. M. (1995). Understanding the radar backscattering from flooded and non-flooded Amazonian forests: Results from canopy backscatter modeling. *Remote Sensing of Environment*, *54*, 324–332.